$E1$ excitations in $A = 15$ nuclei*

M. H. Harakeh† and P. Paul
Physics Department, State University of New York, Stony Brook, New York 11794

H. M. Kuan
Physics Department, Brooklyn College, City University of New York, Brooklyn, New York 11210

E. K. Warburton
Brookhaven National Laboratory, Upton, New York 11973
(Received 13 August 1975)

The $^{14}C(p,\gamma)^{15}N$ reaction was studied from $E_p = 2.8$ to 30 MeV corresponding to $E_x = 13$ to 38 MeV in ^{15}N covering the region of the lowest $T = \frac{3}{2}$ states as well as the giant dipole resonance (GDR). The $^{14}N(p,\gamma)^{15}O$ reaction measurements were extended for excitation regions from $E_x = 24$–33.5 MeV thus covering the analogous regions in ^{15}O and ^{15}N. Angular distributions obtained in the first reaction at the resonance energies of $E_p = 4.83$, 5.62, 6.65, 6.925, 10.0, 11.0, 12.35, 13.6, and 16.4 MeV indicated large negative a_2 coefficients in all cases. The new narrow ($\Gamma_{c.m.} = 90$ keV) resonance at 6.925 MeV has $J^\pi = \frac{3}{2}^+$ and $T = \frac{1}{2}$. A careful comparison of the $^{15}N(\gamma,p_0)^{14}C$ and $^{15}O(\gamma,p_0)^{14}N$ reactions is used to extract the $T = \frac{3}{2}$ and $\frac{1}{2}$ components of the GDR in $A = 15$. Most of the $T = \frac{3}{2}$ $E1$ strength is located near $E_x = 26$ MeV. A microscopic calculation of $J^\pi \leq \frac{5}{2}^+$ states with $T = \frac{1}{2}$ and $\frac{3}{2}$ in a 2h-1p and 1h basis of good isospin gives good agreement with the observed depleted $B(E1)$ values from the lowest $T = \frac{3}{2}$ states and reproduces the location of the collective $T = \frac{3}{2}$ $E1$ states near 26 MeV. It also describes well the distribution of $T = \frac{1}{2}$ collective $E1$ strength. Using this agreement with the theory which contains no adjusted parameters an effective symmetry potential of $U = 28$ MeV is extracted from the isospin energy splitting. This value is smaller than the typical 60 MeV found in heavier nuclei but agrees with a recent model-independent limit and with other cases of $|T_z| = \frac{1}{2}$ nuclei.

[NUCLEAR REACTIONS ^{15}N, $^{14}C(p,\gamma)$, $E_p = 2.8$–30 MeV, measured $d\sigma/d\Omega(90°)$, angular distributions. ^{15}O, $^{14}N(p,\gamma)$, $E_x = 24$–33.5 MeV, measured $d\sigma/d\Omega(90°)$. Calculated 2h-1p, 1h states of $A = 15$ and $B(E1)$. Deduced location of $T = \frac{3}{2}$ and $\frac{1}{2}$ component of GDR and effective symmetry potential.]

I. INTRODUCTION

This paper concludes a systematic study of electric dipole ($E1$) excitations in nuclei around ^{16}O. The aim is twofold: (1) to explain the low-lying (typically depleted) excitations and the collective giant dipole resonances (GDR) quantitatively in the same framework; (2) to clarify the role of isospin in the collective states in nuclei with $|T_z| = \frac{1}{2}$. In the two preceding papers[1,2] (henceforth, referred to as I and II) the $E1$ excitations in ^{17}F have been investigated experimentally and compared to the results of a microscopic calculation which considered two-particle–one-hole (2p-1h) excitations in a basis of good isospin. It was shown that the energies and transition strengths of the low-lying $T = \frac{3}{2}$ states were reproduced by the model simultaneously with the location and strength distribution of the GDR.

We present here the results of a similar investigation on nuclei with $A = 15$, with emphasis on ^{15}N. Microscopically the $T = \frac{3}{2}$ $E1$ excitations based on the ground state are assumed to have 2h-1p character. The calculations can then be carried out using the identical effective interaction parameters employed in I for $A = 17$ and in this sense the theoretical predictions for $A = 15$ contain no new free parameters. In regard to the experimental study of the isospin components of the GDR, the $A = 15$ system is more advantageous than $A = 17$, because of the existence of the $|T_z| = 1$ target ^{14}C. Both isospin components in ^{15}N are populated in the isospin-allowed reaction $^{14}C(p,\gamma_0)^{15}N$. Then, a comparison (with caution) of this reaction with the $^{14}N(p,\gamma_0)^{15}O$ reaction (which should populate only the $T = \frac{1}{2}$ part) allows an identification of the various isospin states in the $A = 15$ GDR.

On the experimental side we have measured the $^{14}C(p,\gamma_0)^{15}N$ reaction in detail over the extended region of $E_x = 13$ MeV ($E_p = 3$ MeV) to $E_x = 38$ MeV ($E_p = 30$ MeV), i.e., the predicted energy of the $1s$-hole state. In addition the excitation function of the $^{14}N(p,\gamma_0)^{15}O$ reaction is extended beyond previous work[3] up to $E_x = 34$ MeV in ^{15}O which per-

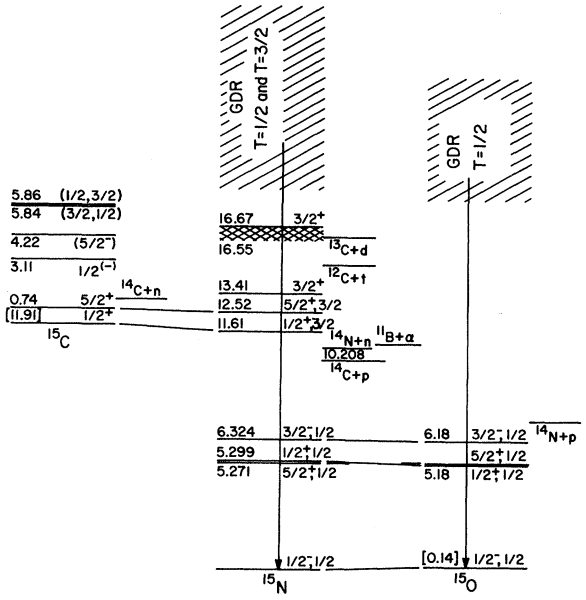

FIG. 1. Level schemes of $A=15$ nuclei relevant to the present discussion. Lines connect established analog states. The assignments of the last two levels in ^{15}C indicate that of the pair one state has $J=\frac{1}{2}$ and the other $J=\frac{3}{2}$. Several relevant particle thresholds are indicated in the proper energy scale.

mits full comparison of the GDR region in ^{15}O and ^{15}N.

Several sets of data are already available on radiative capture into ^{15}N and ^{15}O. The lowest $T=\frac{3}{2}$ states have been extensively measured by Kuan, Umbarger, and Shirk,[4] and the region up in the GDR has been studied by Weller *et al.*,[5,6] in the ^{14}C$(p,\gamma)^{15}$N reaction[5] and in elastic proton scattering[6] on ^{14}C. The inverse photonuclear reaction ^{15}N$(\gamma,p_0)^{14}$C has been studied previously by Kosick.[7] The data presented here disagree in several ways with these previous results (except for the two lowest $T=\frac{3}{2}$ states, at 11.61 and 12.52 MeV, whose γ widths are well established). Figure 1 shows the pertinent states previously identified in ^{15}N and ^{15}O, and the $T=\frac{3}{2}$ parents in ^{15}C. The established ^{15}C levels below 6 MeV excitation are also given with their probable spin-parity assignments.[8] No $T=\frac{3}{2}$ analog states, besides the ground state and first excited state analogs, have been established in the corresponding region of excitation energy in ^{15}N, which are deduced from narrow resonances observed in the ^{14}C(p,γ_0) reaction. Levels at 13.41, 16.55, and 16.67 MeV in ^{15}N are included. These will be discussed in detail later.

In the theoretical part of this paper the results of the 2h-1p calculation will be checked against energies and $E1$ strengths of the lowest $T=\frac{3}{2}$ states. The predictions at higher energies for the collective $T=\frac{3}{2}$ and $\frac{1}{2}$, $\frac{1}{2}^+$, and $\frac{3}{2}^+$ excitations will then be compared to the inverse capture cross sections observed in ^{15}N and ^{15}O.

II. EXPERIMENTAL PROCEDURE AND RESULTS FOR ^{14}C$(p,\gamma_0)^{15}$N

To cover the extended range of the ^{14}C$(p,\gamma)^{15}$N excitation function, the data were taken with two different accelerators but otherwise almost identical detector setups. The bombarding energies for $E_p=2.8$ to 17 MeV were obtained from the Stony Brook tandem while the Brookhaven Double MP tandem was used for the range from $E_p=15$ to 30 MeV. The two sets of data were normalized relative to each other in the 2-MeV region of overlap.

The ^{14}C targets consisted of 95% isotopically enriched layers nominally 100 μg/cm^2 thick deposited on either 0.762-μm Ni or 1.27-μm Au foils and were prepared by Oak Ridge National Laboratory. After early cross section inconsistencies indicated that the real target thickness was less than the nominal value the ^{14}C content was measured directly by elastic proton scattering at $E_p=3.1$ MeV. The elastic yield observed at θ(lab) = 150° was normalized to a cross section value of $d\sigma/d\Omega$(c.m.) = 70 ± 14 mb/sr taken from Ref. 6. This gave a real ^{14}C thickness of 40(±22%) μg/cm^2 for the Au-backed target and all cross sections were subsequently normalized to this target.

The γ rays were detected in 25.4- × 25.4-cm NaI detectors with anticoincidence shields. Two such detectors of almost identical geometry and elec-

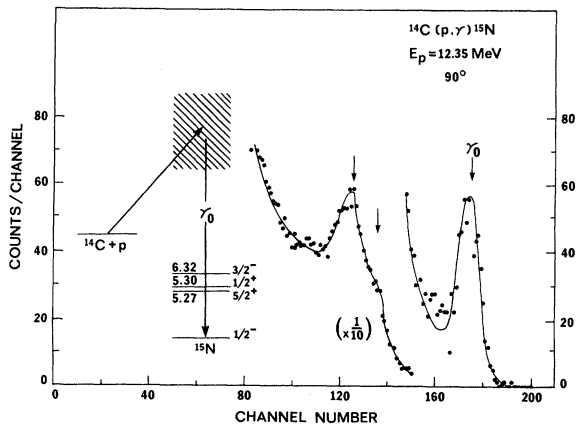

FIG. 2. γ spectrum obtained in the ^{14}C$(p,\gamma)^{15}$N reaction. Arrows indicate the positions of expected γ_0, $\gamma_1+\gamma_2$, and γ_3 transitions. The regions where $\gamma_1+\gamma_2$ and γ_3 appear are contaminated by capture γ rays from the thin Ni backing.

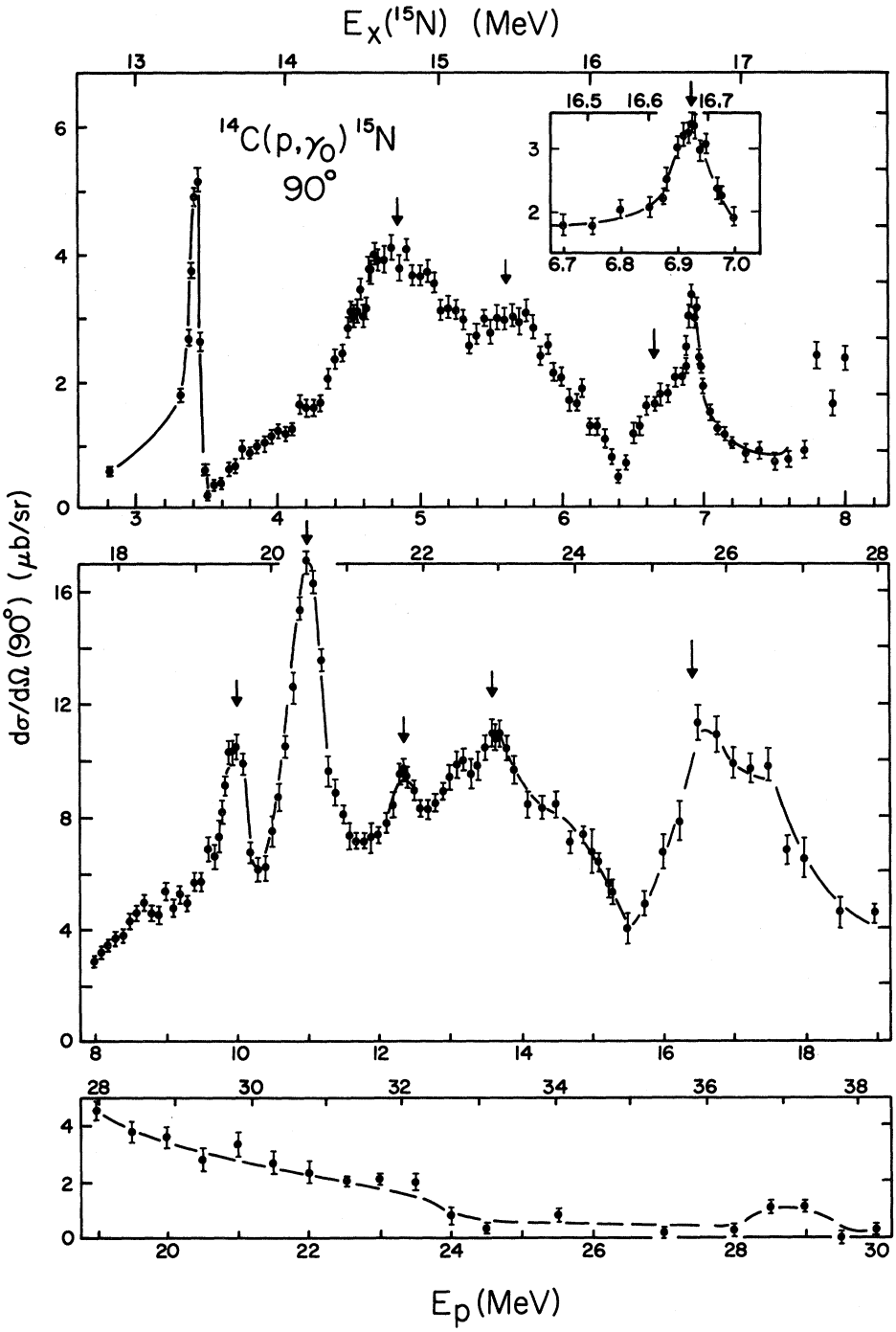

FIG. 3. Excitation function of the $^{14}C(p,\gamma_0)^{15}N$ γ yield at 90°. The top part shows the region where narrow $T=\frac{3}{2}$ resonances may be expected. The insert gives the details of a new resonance at $E_p=6.925$ MeV. The center part shows the region of the GDR and the bottom part the high-energy region up to 30 MeV. Solid lines are drawn to guide the eye. Arrows indicate energies where complete angular distributions were taken.

tronic design were used at BNL and Stony Brook. A typical γ spectrum produced with the Ni-backed target at $E_p = 12.35$ MeV is shown in Fig. 2. The position of the ground-state transition (γ_0) is indicated by the labeled arrow; the other arrows show the positions of possible transitions to the

closely grouped first and second as well as the third excited state. Since these γ-ray groups overlapped in energy with capture γ rays from the Ni and Au backings, transitions to excited states in ^{15}N could not be analyzed meaningfully. The analysis of the γ_0 peak followed standard procedures.[2] Specifically the accepted-to-total ratio curve given in II for the BNL detector was used to establish the real yield.

The absolute cross section scale was established from a run over the strong resonance at $E_p = 1.5$ MeV. The yield at this resonance is essentially isotropic. A peak cross section of 17.5(±40%) μb/sr had previously been reported[4] at $\theta = 90°$. This value was later corroborated by Young, Figuera, and Steerman[9] but was inconsistent with an older measurement.[10] It was therefore decided to make an independent absolute recalibration of this resonance cross section. For this measurement the γ rays were detected in a very well collimated geometry and without any electronic rejection; the front plastic of the detector was removed. Using the target thickness given above, a peak cross section of 16.8(±25%) μb/sr was obtained at $\theta = 90°$ which is in excellent agreement with the previous value.[4] The assigned error stems essentially from the cross section error of the ^{14}C$(p,p)^{14}$C reaction used to establish the target thickness; obviously both the old and the new errors are very conservative.

The γ_0 yield of the ^{14}C$(p,\gamma_0)^{15}$N reaction was then measured at 90° as a function of bombarding energy and the results are plotted in Fig. 3. The low-energy region where narrow $T = \frac{3}{2}$ resonances may be expected (shown in the top part of Fig. 3) was taken in the fine steps of 10 to 50 keV. For the main region of the GDR (center part) the step size was increased to 50–100 keV. Still larger steps were used at the highest-energy region (bottom part). A comparison of this curve to published results[5] on this reaction and the inverse reaction[7] points to some discrepancies in the region of overlap

(i) The resonance peak at $E_p = 3.41$ MeV is followed by a much deeper interference valley than shown in the data of Ref. 5.

(ii) In the region $E_p = 3.5$ to 16 MeV there are many differences in detail with Ref. 5, such as relative height and peak-to-valley ratios at the resonances near 4.8, 5.8, 6.8, and 9.95 MeV as well as in the lower part of the GDR.

(iii) A new narrow resonance is observed at $E_p = 6.925$ MeV in the present data (see insert in Fig. 3). The excitation energy $E_x = 16.67$ MeV and its total width of $\Gamma_{c.m.} = 90 \pm 10$ keV agree closely with that of a resonance recently reported[11] in the ^{12}C$(t,\gamma_0)^{15}$N reaction.

(iv) In the main portion of the GDR the present excitation function resembles, in general, that of the inverse ^{15}N$(\gamma,p_0)^{14}$C reaction but again differs in some details, specifically the peak near $E_x = 26$ MeV which appears at 24.6 MeV in the published[7] ^{15}N$(\gamma,p_0)^{14}$C data. A very new measurement[12] seems to confirm our data. This peak is important for the isospin splitting of the GDR since it will be shown to contain most of the $T = \frac{3}{2}$ strength.

(v) In the highest energy region a small peak was consistently observed in the present data near $E_p = 29$ MeV corresponding to an excitation energy of 37 MeV. This is close to the expected location of the $1s_{1/2}^{-1}$ state.

Angular distributions were then measured on various peaks, at $E_p = 4.83$, 5.62, 6.65, 6.925, 10.0, 11.0, 12.35, 13.6, and 16.4 MeV. The results were in major disagreement with those reported before at the same peaks,[5] and even with some recent results.[12] Therefore, the isotropy of the detection geometry was checked carefully by taking an angular distribution at $E_p = 1.6$ MeV, at the upper shoulder of the $J^\pi = \frac{1}{2}^+$ resonance. At this energy previous work[4,10] has shown the angular distribution to be isotropic with very little interference from the resonances below 1.5 MeV. Our results confirm this. The present results are collected in Fig. 4, including fits with sums of Legendre polynomials up to and including P_3. Except at 1.6 MeV, no distribution is isotropic.

The extracted total cross section $4\pi A_0$ and the normalized Legendre coefficients $a_i = A_i/A_0$ are plotted on the right hand side of Fig. 4 as a function of energy. The coefficients at the resonances $E_p = 4.83$, 5.62, and 6.65 MeV are in disagreement with previous work.[5] All resonances (except at 1.6 MeV) have large a_2 coefficients. Thus none of the peaks shown in Fig. 4 corresponds to an isolated state with $J = \frac{1}{2}$, although $J = \frac{1}{2}$ and $\frac{3}{2}$ resonances might overlap. For instance, the peak at 4.83 MeV could perhaps be predominantly $J = \frac{1}{2}$ with a tail interference from the 5.62-MeV $J = \frac{3}{2}$ resonance. The largest anisotropy $a_2 = -0.74$ is observed at the 6.925-MeV resonance. Assuming dipole radiation for the decay this requires $J = \frac{3}{2}$ for the narrow resonance and interference with a background of the same spin. The angular distribution at the broader peak just below, at $E_p = 6.65$ MeV, indeed indicates $J = \frac{3}{2}$ for this resonance, too.

If the top part of Fig. 3 is fitted with the smallest number of Breit-Wigner curves one obtains a good fit with resonances at 3.41 MeV [Γ(lab) = 60 keV], 4.0 MeV, (broad), 4.83 MeV (800 keV), 5.62 MeV (800 keV), 6.70 MeV (600 keV), and 6.925 MeV (100 keV). Many positive-parity resonances over this region have been reported from the reac-

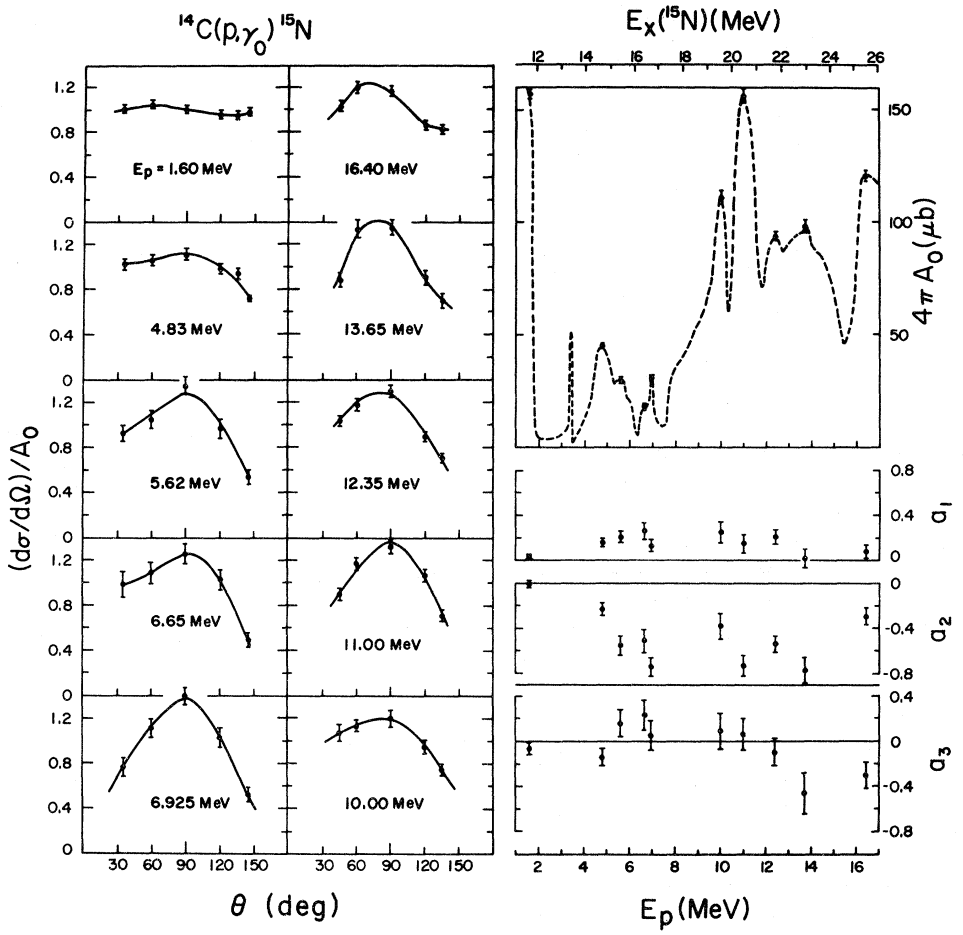

FIG. 4. Normalized angular distributions of the γ_0 yield at several bombarding energies corresponding to peaks in the excitation function. The curve at E_p=1.6 MeV should be isotropic. Solid curves are fits with Legendre polynomials up to P_3. The total cross section $4\pi A_0$ and the normalized Legendre coefficients a_1, a_2, a_3 obtained from the fits are plotted on the right hand side of the figure.

tions[6,13] $^{14}C(p,p)^{14}C$ and $^{14}C(p,\alpha)^{11}B$. There appears to be little correspondence (except at $E_p = 3.41$ MeV) between peaks reported in the particle reactions and the present radiative capture data.

III. EXPERIMENTAL RESULTS FOR THE $^{14}N(p,\gamma_0)^{15}O$ REACTION

The excitation function of this reaction has been already measured[3] carefully up to an excitation energy of 25 MeV in ^{15}O. This stops just short of the major peak (see Fig. 3) at $E_x = 26$ MeV observed in ^{15}N in the $^{14}C(p,\gamma_0)$ reaction. In order to permit complete comparison between both reactions, the $^{14}N(p,\gamma_0)^{15}O$ excitation function was extended up to the limits of the BNL three-stage tandem, or an excitation energy of 33.5 MeV. The target used in these runs was an extended gas cell with thin entrance and exit window, filled with natural N_2 gas. Details of the cell and the detection geometry have been described elsewhere.[2] The γ_0 yield observed at $\theta = 90°$ was normalized to the cross section data of Kuan *et al.*[3]

IV. MICROSCOPIC CALCULATION OF $E1$ EXCITATIONS IN ^{15}N

A. Introduction

We compute here the $J \leq \frac{5}{2}$ states of positive parity for $A = 15$ in a 2h-1p basis of good isospin following the procedures outlined in I for $A = 17$. As in the case of $A = 17$, the low-lying $T = \frac{1}{2}$ positive-parity states of $A = 15$ nuclei have already been the subject of many shell model calculations. Some of these states were successfully described in a 2h-1p basis, but it became obvious that 4h-3p configurations had to be involved[14,15] to explain the positive-parity states below 10 MeV. Good agreement with experiment was obtained by Lie, Engeland, and

Dahll[16] in explaining the level energies and their γ-decay properties.

Much less theoretical work has been reported for the lowest $T=\frac{3}{2}$ states. Zuker, Buck, and McGrory[17] calculated the first $\frac{1}{2}^+$ and $\frac{5}{2}^+$ $T=\frac{3}{2}$ states assuming a closed ^{12}C core and three valence nucleons free to occupy $1p_{1/2}$, $1d_{5/2}$, and $2s_{1/2}$ orbitals. Soga[18] calculated the same states assuming a weak coupling of a $2s_{1/2}$ or $1d_{5/2}$ particle to the $J^\pi=0^+$ $(T=1)$ 2h ground state of ^{14}C. He obtained very good agreement with the experimental level energies.

The collective states which emerge from the 2h-1p basis have been calculated recently by Fraser, Garnsworthy, and Spicer[19] with two types of residual interaction: (1) a Gillet type interaction and (2) a zero-range force with adjustable strength parameter. In particular, they predict the main strength of the $T=\frac{3}{2}$ GDR in $A=15$ to lie at 26 MeV excitation.

The present approach is to calculate the low-lying $T=\frac{3}{2}$ states and the collective $T=\frac{1}{2}$ and $T=\frac{3}{2}$ states simultaneously using realistic p-p and p-h residual interactions derived from the phenomenological Hamada-Johnston potential. Since the same effective matrix elements are used which already successfully explained the $E1$ excitations in $A=17$, no new free parameters are involved in the $A=15$ calculations.

B. Computation of the 2h-1p states and their $E1$ transition strengths

For the computation of the positive-parity states with $J\leq\frac{5}{2}$ in a 2h-1p basis the entire $1p$ and $(2s, 1d)$ shells were taken as active for the holes and particles, respectively. The Hamiltonian of this system is

$$H=\sum_\alpha \epsilon_\alpha(a_\alpha^\dagger a_\alpha+b_\alpha^\dagger b_\alpha)+\sum_{\alpha\beta\gamma\delta} V^{\rm hh}_{\alpha\beta\gamma\delta}b_\alpha^\dagger b_\beta b_\delta b_\gamma + \sum_{\alpha\beta\gamma\delta} V^{\rm ph}a_\alpha^\dagger b_\beta^\dagger b_\delta a_\gamma,$$

where the notation defined in I has been used; $V^{\rm hh}$ is the hole-hole interaction, $V^{\rm ph}$ the particle-hole interaction.

The 2h-1p basis states were constructed in the j-j formalism, such that

$$|j_\alpha^{-1}j_\beta^{-1}(J_1T_1), j_\gamma; JT\rangle=[[b_\alpha^\dagger b_\beta^\dagger]_{J_1T_1}a_\gamma^\dagger]_{JT},$$

i.e., the wave functions of the two holes (α,β) in the $1p$ shell are coupled and antisymmetrized to a state of total angular momentum J_1 and isospin T_1. The wave function of the particle γ in the $(2s, 1d)$ shell is then coupled to the two-hole state to form the 2h-1p state with total angular momentum J and isospin T.

In principle, the one-hole configuration must be added for the $T=\frac{1}{2}$ states. However, mixing of the $1s_{1/2}$-hole configuration (the only one possible) with the 2h-1p states was disregarded. This 1h state is expected to be weakly mixed with the 2h-1p configurations since such mixture would involve wave functions of three major shells whose overlap is small. Thus the dipole strength of the $(1s)$-hole state should occur essentially at the unperturbed energy of a $1s$ hole in ^{16}O. Relative to the ^{15}N ground state this excitation should be[19] around 36 MeV.

The unperturbed energies for the single-particle (s.p.) and single-hole (s.h.) orbitals were identical to those listed in I and were taken from the experimental level spectra of nuclei around ^{16}O. The p-h matrix elements are the same as those used in I and were derived from the Kuo-Brown p-p matrix elements.[20] The h-h matrix elements are derived from the p-p matrix elements in the $(1p)$ shell using the relation

$$\langle j_a^{-1}j_b^{-1}JT)|V^{\rm hh}|j_c^{-1}j_d^{-1}JT\rangle=\langle j_c j_d JT|V^{\rm pp}|j_a j_b JT\rangle.$$

For the p-p interaction in the $(1p)$ shell two sets of matrix elements were considered: (i) the realistic Kuo-Brown matrix elements derived from the Hamada-Johnston potential,[20] hereafter referred to as case A, and (ii) the Cohen-Kurath effective two-body p-p matrix elements[21] obtained from fitting energy data of $(1p)$ shell nuclei and adjusted with respect to a ^{16}O core. This will be called case B in the text.

Here, as in I, the Coulomb interaction was disregarded. The spurious center of mass effects which enter into the $T=\frac{1}{2}$ states were removed following the approximate procedure of Giraud.[22] It should be pointed out that this procedure is probably quite good here since we are not interested in the low-lying $T=\frac{1}{2}$ states.

The $E1$ decay transition strengths of the 2h-1p states to the ground state $(\frac{1}{2}^-)$ and third excited state $(\frac{3}{2}^-)$ at 6.3 MeV in ^{15}N were computed with the assumption of single-hole character $1p_{1/2}^{-1}$ and $1p_{3/2}^{-1}$, respectively, for the final states. Thus one obtains

$$B(E1)=\frac{1}{(2J_i+1)}\left|\sum_{bcd}\sum_{J_1T_1}\langle j_b^{-1}j_c^{-1}(J_1T_1), j_d; J_iT_i|\phi_i^{J_iT_i}\rangle\langle\phi_f^{J_fT_f}\|\tilde{E}1\|j_b^{-1}j_c^{-1}(J_1T_1), j_d; J_iT_i\rangle\right|^2$$

with a self-explanatory notation. The reduced matrix elements contained in the last equation were evalu-

ated according to

$$\langle j_a^{-1}\|\tilde{E}1\|j_b^{-1}j_c^{-1}(J_1T_1),j_d;JT\rangle=(-)^{j_b+j_d}C_{T1}(\tfrac{1}{2}-\tfrac{1}{2};-\tfrac{1}{2}0)W(T_1\tfrac{1}{2}\tfrac{1}{2}1;T\tfrac{1}{2})\left(\frac{9}{16\pi}\right)^{1/2}(\hat{J}_1\cdot\hat{T}_1\cdot\hat{J}\cdot\hat{T}\cdot\hat{j}_d\cdot\hat{l}_d)^{1/2}$$
$$\times\Big[\delta j_a j_b(1+\delta_{j_b j_c})^{1/2}\hat{j}_b^{1/2}C_{l_d}1(l_b0;00)W(J_1j_dj_c1;Jj_b)W(\tfrac{1}{2}l_dj_b1;j_dl_b)$$
$$\times\int R^{l_b}_{n_b}(r)R^{l_d}_{n_d}(r)r^2dr-(-1)^{J_1+T_1}\delta_{j_aj_b}(1-\delta_{j_bj_c})^{1/2}(\delta\hat{j}_c)^{1/2}C_{l_d}1(l_c0;00)$$
$$\times W(J_1j_dj_b1,Jj_c)W(\tfrac{1}{2}l_dj_c1;j_dl_c)\int R^{l_c}_{n_c}(r)R^{l_d}_{n_d}(r)r^2dr\Big],$$

where C and W are Clebsch-Gordan and Racah coefficients $\hat{j}=2j+1$ and harmonic oscillator wave functions with $\hbar\omega=41A^{-1/3}$ MeV were used in the radial integrals.

C. Comparison of theoretical results and experiments for the lowest $T=\frac{3}{2}$ states

In Fig. 5 the calculated $T=\frac{3}{2}$ level spectra obtained from cases A and B are compared to the experimentally known $T=\frac{3}{2}$ levels in ^{15}N and to Soga's predictions.[18] For comparison, the known low-lying levels of ^{15}C are also shown. Obviously case B (which contains a more realistic hole-hole interaction) gives better agreement with the experimental level energies than case A. Both cases, however, give the correct ordering for the first $\frac{1}{2}^+$ and $\frac{5}{2}^+$ levels. They also predict a $J=\frac{3}{2}^+$, $T=\frac{3}{2}$ state between 16 and 17 MeV of excitation. A doublet is indeed observed[8] at nearly equivalent energy in ^{15}C in the reaction ^{9}Be(^{7}Li, p)^{15}C with proposed spins of $\frac{1}{2}$ and $\frac{3}{2}$ but uncertain parity. The analog states in ^{15}N have not yet been assigned. Evidence for a $T=\frac{3}{2}$ state at the proper energy in the radiative capture data will be discussed later.

Soga's calculation, despite its more limited basis, reproduces the positions of the lowest $\frac{1}{2}^+$ and $\frac{5}{2}^+$ ($T=\frac{3}{2}$) states in ^{15}N very well. Comparison with the present results from the complete 2h-1p basis confirms his earlier conjecture that these states consist of $2s_{1/2}$ and $1d_{5/2}$ particles weakly coupled to a $J=0^+$ $T=1$ 2h state (i.e., the ^{14}C ground state). Table I gives the wave function for the lowest $\frac{1}{2}^+$, $\frac{5}{2}^+$, $\frac{3}{2}^+$ ($T=\frac{3}{2}$) states from cases A and B and includes Soga's results for the first two. Manifestly, these three states are rather pure $d_{5/2}$, $s_{1/2}$, $d_{3/2}$ weak-coupling states. However, some of the additional terms in the wave functions carry very large $E1$ matrix elements.

The results for the $E1$ transition strengths can be seen from Table II where the $B(E1)$ values are listed for transitions from all three states to various allowed $T=\frac{1}{2}$ final states. No reduced rates were given in Soga's paper, so those listed in Table II were computed here from his wave functions. The transition rate for the decay of the $\frac{1}{2}^+$ $T=\frac{3}{2}$ state to the $\frac{1}{2}^-$ ground state of ^{15}N computed[4] from the wave function of Zuker *et al.*[17] (ZBM) appears in the last column. Since the ZBM

TABLE I. Wave functions of the lowest $T=\frac{3}{2}$ states $\frac{1}{2}^+$, $\frac{5}{2}^+$, and $\frac{3}{2}^+$ in 2h-1p configurations. Amplitudes less than 0.1 are deleted and others are zero for obvious geometrical reasons.

Configuration 2h(J, T)⊗1p	$\frac{1}{2}^+$ Case A	$\frac{1}{2}^+$ Case B	$\frac{1}{2}^+$ Soga	$\frac{5}{2}^+$ Case A	$\frac{5}{2}^+$ Case B	$\frac{5}{2}^+$ Soga	$\frac{3}{2}^+$ Case A	$\frac{3}{2}^+$ Case B
$1p_{3/2}^{-2}(0,1)\otimes 1d_{5/2}$				0.32	0.42	0.39		
$1p_{3/2}^{-2}(0,1)\otimes 2s_{1/2}$	0.27	0.37	0.39					
$1p_{3/2}^{-2}(0,1)\otimes 1d_{3/2}$							0.24	0.25
$1p_{3/2}^{-1}1p_{1/2}^{-1}(1,1)\otimes 1d_{5/2}$							−0.15	−0.11
$1p_{3/2}^{-1}1p_{1/2}^{-1}(2,1)\otimes 1d_{5/2}$	−0.21	−0.17		−0.33	−0.25		−0.18	−0.16
$1p_{3/2}^{-1}1p_{1/2}^{-1}(1,1)\otimes 2s_{1/2}$							0.19	0.11
$1p_{3/2}^{-1}1p_{1/2}^{-1}(2,1)\otimes 2s_{1/2}$							−0.19	−0.13
$1p_{3/2}^{-1}1p_{1/2}^{-1}(2,1)\otimes 1d_{3/2}$							−0.24	−0.21
$1p_{1/2}^{-2}(0,1)\otimes 1d_{5/2}$				0.88	0.86	0.92		
$1p_{1/2}^{-2}(0,1)\otimes 2s_{1/2}$	0.94	0.91	0.92					
$1p_{1/2}^{-2}(0,1)\otimes 1d_{3/2}$							0.86	0.87

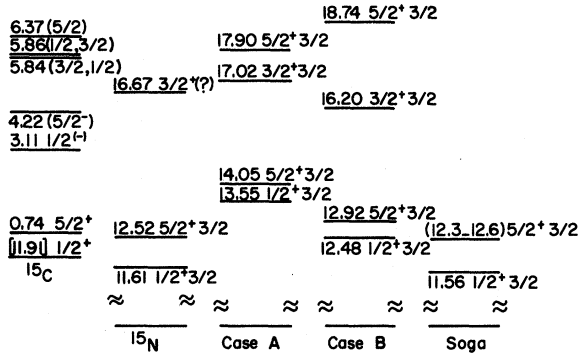

FIG. 5. Experimental and computed spectrum of $T = \frac{3}{2}$ positive-parity levels with $J \leq \frac{5}{2}$. For comparison the low-lying levels in ^{15}C are also shown (taken from Ref. 8). Levels are labeled by J^π, T and probable assingments are in brackets. Cases A and B are the predictions of the present calculations, the final column is a previous results by Soga (Ref. 18). All calculations are described in the text.

model space contained a closed ^{12}C core no transitions are possible to the $\frac{3}{2}^-$ excited state. Experimental $B(E1)$ values are also listed where available.[4,23]

In Soga's calculations each transition is produced by only a single matrix element. The reduced transition rates are thus the s.p. values multiplied by the appropriate coefficients (squared) listed in Table I. Hence, the depletion in strength is due to the reduction in amplitude of the one component in the wave function which can make an $E1$ transition. In cases A and B a further reduction in strength is the result of destructive interference of different matrix elements. In the case of the $\frac{1}{2}^+ \rightarrow \frac{1}{2}^-$ transition in ^{15}N this reduction seems to be more than demanded by the data, although an experimental value given for the analogous transition[23] in ^{15}O is in better agreement with A and B. In fact, this discrepancy of two $E1$ decay widths in analogous transitions is quite suspicious and was one of the reasons why the resonance cross section for this transition was carefully remeasured in ^{15}N. All other listed transitions show remarkable agreement between experiment and the present calculations.

D. Predictions for the collective states

Having successfully tested the wave functions against the data for the low-lying $E1$ excitations we wish now to list the predictions for the collective states which emerge from the same diagonalization. Tables III and IV list the $B(E1\downarrow)$ values, i.e., those for decay to the ground state, which result from cases A and B, respectively, and which exceed 0.02 $e^2\,\mathrm{fm}^2$. $T = \frac{1}{2}$ and $\frac{3}{2}$ states are listed separately. The predictions of A and B are quite similar and indicate giant resonances located at energies between 20 and 26 MeV.

Finally, in Table V the collective $E1$ excitations based on the $1p_{3/2}{}^{-1}$ third excited state (at 6.3 MeV excitation) are listed for completeness as they are obtained from cases A and B. Comparison with the results of Table II and III shows the GDR built on the $1p_{3/2}{}^{-1}$ state to be shifted up in excitation energy by about 6 MeV from those built on the ground state. This bears out the weak-coupling model where the collective $E1$ states in ^{16}O are coupled to the single-hole excitations of the respective basis states in the $A = 15$ nucleus. No experimental data are available on the $E1$ excitations from the 6.3-MeV state in ^{15}N.

In Table VI some experimentally important

TABLE II. Experimental and calculated reduced $E1$ transition rates, in units of $e^2\,\mathrm{fm}^2$, from the lowest $T = \frac{3}{2}$ states with $J^\pi = \frac{1}{2}^+$, $\frac{5}{2}^+$, and $\frac{3}{2}^+$, to the ground state ($\frac{1}{2}^-$) and the third excited state ($\frac{3}{2}^-$) of ^{15}N.

Initial state J^π, T	Final state E_x (MeV)	J^π	Reduced transition rates Exp.[a]	Theory Case A	Case B	Soga	ZBM[a]
$\frac{1}{2}^+$, $\frac{3}{2}$	0	$\frac{1}{2}^-$	0.030 ± 0.012 (0.010 ± 0.003)[b]	0.009	0.013	0.056	0.0683
	6.33	$\frac{3}{2}^-$	0.0065 ± 0.0052	0.003	0.005	0.010	···
$\frac{5}{2}^+$, $\frac{3}{2}$	0	$\frac{1}{2}^-$		0	0	0	0
	6.33	$\frac{3}{2}^-$	0.0015 ± 0.0008	0.001	0.004	0.015	···
$\frac{3}{2}^+$, $\frac{3}{2}$	0	$\frac{1}{2}^-$		0.011	0.026		
	6.33	$\frac{3}{2}^-$		0.0003	0.0001		

[a] See Ref. 4.
[b] See Ref. 23.

TABLE III. Case A calculation. Reduced transition rates $B(E1\downarrow)$ for dipole states in ^{15}N (those $\geq 0.02\ e^2\text{fm}^2$ are listed).

$\frac{1}{2}^+$		$\frac{3}{2}^+$	
E_x (MeV)	$B(E1\downarrow)$ (e^2fm^2)	E_x (MeV)	$B(E1\downarrow)$ (e^2fm^2)
	$T=\frac{1}{2}$		
21.07	0.17	16.61	0.02
21.62	0.08	18.38	0.07
23.21	0.05	18.66	0.04
25.02	0.04	20.23	0.11
26.95	0.02	22.58	0.07
		23.61	0.02
		25.81	0.02
		28.88	0.02
	$T=\frac{3}{2}$		
23.45	0.48	20.04	0.02
24.77	0.08	21.29	0.03
		23.96	0.57
		27.95	0.03
		32.59	0.02

quantities are extracted from the microscopic calculations and compared to model-independent predictions for the GDR in $A=15$. Both A and B yield bremsstrahlung-weighted cross sections[24] σ_{-1} which agree with the Levinger estimate of $0.36\times A^{4/3}$. The total absorption cross section obtained from the microscopic model exceeds the classical dipole sum rule by a factor 1.3. This was also found[1] in $A=17$ and is quite typical.

TABLE IV. Case B calculation. Reduced transition rates $B(E1\downarrow)$ for dipole states in ^{15}N (those $\geq 0.02\ e^2\text{fm}^2$ are listed).

$\frac{1}{2}^+$		$\frac{3}{2}^+$	
E_x (MeV)	$B(E1\downarrow)$ (e^2fm^2)	E_x (MeV)	$B(E1\downarrow)$ (e^2fm^2)
	$T=\frac{1}{2}$		
21.23	0.16	15.27	0.03
22.39	0.13	17.69	0.02
23.68	0.02	18.92	0.05
26.23	0.05	20.67	0.15
		22.29	0.03
		23.18	0.03
		25.33	0.02
		25.95	0.03
	$T=\frac{3}{2}$		
24.30	0.43	16.20	0.03
25.73	0.11	21.19	0.02
29.73	0.03	22.33	0.05
		24.86	0.50
		28.96	0.03
		32.04	0.02
		33.33	0.02

An essential aspect of this investigation is the isospin distribution in the collective $E1$ states. The microscopically obtained $\sigma_{-1}(T=\frac{3}{2})$ fraction of 0.62 agrees well with two estimates based on sum rules.[25,26] The energy separation of the $T=\frac{3}{2}$ and $\frac{1}{2}$ strength may be obtained from $\Delta E = E(\frac{3}{2}) - E(\frac{1}{2}) = (U/A)(T_0+1) = U/10$. The effective symmetry potential $U=60$ predicted by Aküyz and Fallieros[27] was found to work well in heavier nuclei.[28] Leonardi[29] has a much smaller estimate of $U=14$ MeV. Our results fall in between. They are very close to a model-independent upper limit of $U=28$ which has recently been given for $|T_z|=\frac{1}{2}$ nuclei.[30] It is notable that the microscopic values for both $A=17$ and 15 lie close to the upper bound.

Fraser *et al.*[19] obtain very similar results for the collective $E1$ excitations if an appropriate strength parameter is chosen. We point out again that the present results contain no adjustable parameters.

V. DISCUSSION OF THEORY AND EXPERIMENT

To facilitate comparison of the computed $E1$ excitations with the radiative capture cross sections in the $A=15$ system, the capture cross sections of the ^{14}C$(p,\gamma_0)^{15}$N and ^{14}N$(p,\gamma_0)^{15}$O reactions were inverted using detailed balance and are plotted in

TABLE V. GDR states built on the third excited $(1p_{3/2}^{-1})$ state in $A=15$ from cases A and B [only $B(E1\downarrow) \geq 0.04\ e^2\text{fm}^2$ are listed].

$\frac{1}{2}^+$		$\frac{3}{2}^+$		$\frac{5}{2}^+$	
E_x (MeV)	$B(E1\downarrow)$ (e^2fm^2)	E_x (MeV)	$B(E1\downarrow)$ (e^2fm^2)	E_x (MeV)	$B(E1\downarrow)$ (e^2fm^2)
		Case A $T=\frac{1}{2}$			
26.95	0.13	25.81	0.08	25.06	0.06
29.46	0.15	28.88	0.07	29.44	0.24
31.88	0.09	29.14	0.07		
		30.69	0.07		
		Case A $T=\frac{3}{2}$			
25.47	0.04	25.69	0.06	29.70	0.49
28.95	0.26	29.65	0.60	33.50	0.12
33.06	0.13				
		Case B $T=\frac{1}{2}$			
25.09	0.09	22.29	0.04	22.94	0.05
27.11	0.17	24.27	0.04	27.93	0.26
30.58	0.09	27.73	0.17		
		29.49	0.04		
		32.30	0.04		
		Case B $T=\frac{3}{2}$			
26.47	0.04	26.68	0.08	30.65	0.44
29.73	0.29	30.73	0.57	34.69	0.14
33.82	0.11				

TABLE VI. Summary of theoretical results.

	General rules	2h-1p calc. Case C	2h-1p calc. Case D
$\sigma_0=\int\sigma dE$ (MeV mb)	$=60NZ/A$ $=224$	$\sigma_0(\text{tot})=291$	$\sigma_0(\text{tot})=295$
$\sigma_{-1}=\int(\sigma/E)dE$ (mb)	$=0.36A^{4/3}$ $=13.3$	$\sigma_{-1}(\text{tot})=12.6$	$\sigma_{-1}(\text{tot})=12.5$
$\sigma_{-1}(T+1)/\sigma_{-1}$	0.58 [a]; 0.59 [b]	0.62	0.62
$E_{\text{GDR}}=\sigma_0/\sigma_{-1}$ (MeV)		$E_{T=1/2}=21.7$ $E_{T=3/2}=23.9$	$E_{T=1/2}=21.9$ $E_{T=3/2}=24.7$
$\Delta E=E_{T=3/2}-E_{T=1/2}$ (MeV)	$=U(T_0+1)/A$ $=6.0$ ($U=60$ MeV) [c] $=1.4$ ($U=14$ MeV) [d]	2.2 $\Rightarrow(U=22$ MeV)	2.8 $\Rightarrow(U=28$ MeV)

[a] See Ref. 25.
[b] See Ref. 26.
[c] See Ref. 27.
[d] See Ref. 29.

Fig. 6 as a function of γ-ray energy. The theoretical integrated absorption cross sections proportional to $E_\gamma[B(E1\downarrow)]$ are given in the lower half.

A. Excitations between 10 and 20 MeV

The states of most interest in this region are those $T=\frac{3}{2}$ states with a s.p. coupled weakly to the ^{14}C ground state. The first two $T=\frac{3}{2}$ resonances observed in $^{14}\text{C}(p,\gamma_0)^{15}\text{N}$ at $E_p=1.5$ and 2.482 MeV are unambiguously assigned as the $2s_{1/2}$ and $1d_{5/2}$ weak-coupling states[4,8] (see Fig. 1). Figure 5 and Table II indicate the good agreement for energy and transition strength between our theory and experiment. The $1d_{3/2}$ state is predicted at 16.2 MeV (case B) or 17.02 MeV (case A) by the calculations. A simple weak-coupling estimate based on the level scheme of ^{17}O would put this state at 17.52 MeV in ^{15}N.

The narrow resonance at $E_p=3.41$ MeV ($E_x=13.42$ MeV) has been suggested[31] as a $T=\frac{3}{2}$ state and from the (p,γ) angular distribution it has $J=\frac{3}{2}$. However, no suitable parent analog has been found in ^{15}C in any suitable reaction,[8] and no γ transitions to possible antianalog states were found[32] in ^{15}N. The state has a sizeable α width[13] ($\Gamma_\alpha/\Gamma\approx0.1$). It has most likely $T=\frac{1}{2}$. Our calculations predict a $J^\pi=\frac{3}{2}^+$ $T=\frac{1}{2}$ state at 12.9 MeV with a reduced transition rate $B(E1\downarrow)=0.0009$ e^2 fm^2 and with very little overlap in the $^{14}\text{C}+p$ channel. The experimentally observed $B(E1\downarrow)$ value for the 13.42-MeV state is 0.0012 ± 0.0004 e^2 fm^2, in rather good agreement.

The new narrow resonance at $E_p=6.925$ MeV ($E_x=16.67$ MeV) would be an excellent candidate for the $1d_{3/2}$ $T=\frac{3}{2}$ state, as Fig. 1 shows possible parent states (although of unknown parity) exist in ^{15}C. The (p,γ) angular distribution gives $J=\frac{3}{2}$ for the resonance. However, this resonance appears strongly in the $^{12}\text{C}+t$ channel[11] which rules out a $T=\frac{3}{2}$ assignment. At this high excitation $T=\frac{3}{2}$ states need no longer be narrow. However, the nearest peak ($\Gamma_{\text{c.m.}}=550$ keV) centered at $E_p=6.65$ MeV appears to be also present in the $^{12}\text{C}+t$ channel and thus would have $T=\frac{1}{2}$. A comparison with ^{15}C (see Fig. 1) suggests that the $d_{3/2}$ $T=\frac{3}{2}$ state should not be at a lower energy in ^{15}N. The present calculations predict a second $J=\frac{3}{2}^+$ $T=\frac{1}{2}$, state at an energy $E_x=16.7$ MeV with a $B(E1\downarrow)$ value of 0.003 e^2 fm^2 and very small overlap with the $^{14}\text{C}+p$ channel. The published data on $^{14}\text{C}(p,p)$-^{14}C which do not in general show much correspondence with the $^{14}\text{C}(p,\gamma)$ data, indicate a resonance at $E_p=7.00$ MeV with $J=\frac{3}{2}^+$ $\Gamma=140$ keV and $\Gamma_p/\Gamma=0.12$.

The only other states observed in ^{15}C up to 5.8 MeV probably have negative parity and would be weak in radiative capture. A careful search around $E_p=4.5$ MeV gave no evidence for the analog to the 3.11-MeV $\frac{1}{2}^-$ state of ^{15}C. Indirectly, this supports the negative-parity assignment.

B. Giant resonance region

The GDR in the $A=15$ systems displays several distinct and sharp peaks as is typical for light nuclei. Specifically, two sharp peaks are present in the $^{14}\text{C}+p$ channel around 19.5 and 20.5 MeV while only a weak peak is observed in the $^{14}\text{N}+p$ channel at 20.5 MeV. A strong peak is seen at 26 MeV in $^{14}\text{C}+p$ which is entirely absent in $^{14}\text{N}+p$. When such differences are used to infer isospin assignments the structural difference of ^{14}C and ^{14}N must be considered. This can make a larger difference in the radiative capture yield $\Gamma_p\Gamma_\gamma/\Gamma$ even if both channels are isospin allowed. In general, such sharp peaks in the GDR region are not thought to be related to a particular particle-hole

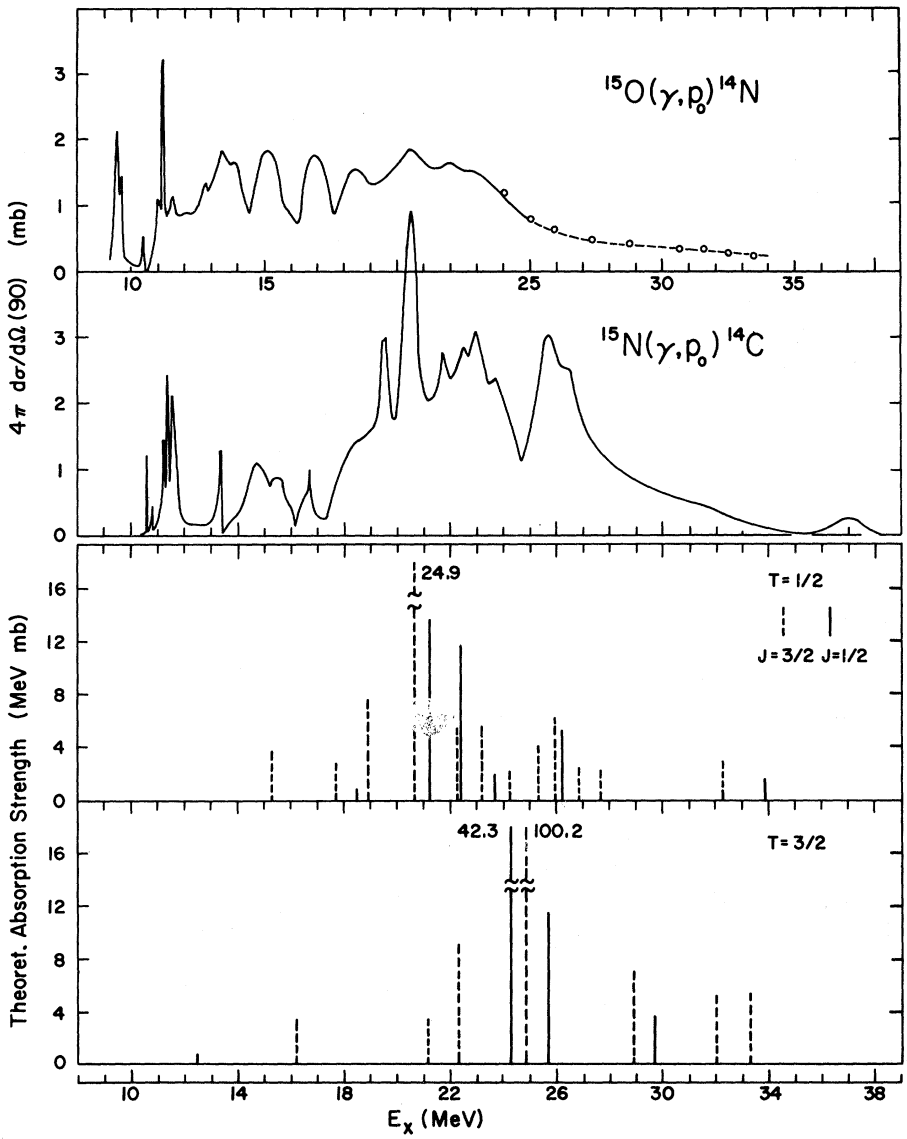

FIG. 6. Comparison of the experimental results from the $^{15}O(\gamma, p_0)^{14}N$ and $^{15}N(\gamma, p_0)^{14}C$ reactions and the theoretical predictions from the 2h-1p model (case B). The data below 25 MeV in the top curve are from Ref. 4, the data points at higher energies stem from the present work. The theoretical plots give the $T=\frac{1}{2}$ and $\frac{3}{2}$ components of the computed integrated photoabsorption cross section proportional to $E_\gamma[B(E1\uparrow)]$. Dashed and solid lines indicate $J=\frac{3}{2}$ and $\frac{1}{2}$, respectively. The top experimental curve should relate to the $T=\frac{1}{2}$ part while the $^{15}N(\gamma, p_0)^{14}C$ curve contains both T components.

component of the collective excitation. Some data on polarized-proton scattering on ^{14}C have been interpreted[33] in terms of a 4-MeV wide $d_{3/2}$ resonance at 19.5 MeV. Obviously, the 19.5-MeV peak observed in the (p,γ) data is much narrower than 4 MeV.

It is apparent from Fig. 6 that the predicted $T=\frac{1}{2}$ strength distribution reproduces the main strength of the $^{15}O(\gamma,p_0)^{14}N$ channel and agrees with the lower part of the GDR peak in the $^{15}N(\gamma, p_0)^{14}C$ channel. The $T=\frac{3}{2}$ strength is predicted to be concentrated in essentially one state each for $J=\frac{1}{2}$ and $\frac{3}{2}$, at 24.3 and 24.9 MeV, respectively. This corresponds reasonable well with the peak at 26 MeV in $^{14}C+p$ channel. Although these two predicted states exhaust ~50% of the total dipole sum rule, they are observed relatively weakly (compared to the bulk of the GDR) in the capture reaction. The structure of these states is mainly (>50%) of the configuration

$$[1p_{3/2}^{-1}1p_{1/2}^{-1}](J=2, T=1)\times 1d_{5/2}$$

and

$$[1p_{3/2}^{-1}1p_{1/2}^{-1}](J=1, T=1)\times 1d_{5/2}$$

for $J=\frac{1}{2}$ and $J=\frac{3}{2}$, respectively. Thus they have little overlap with the ^{14}C ground state, since only a $d_{3/2}$ particle can couple to the ^{14}C ground state to form a $J=\frac{3}{2}^+$ state (or an $s_{1/2}$ particle for a $J=\frac{1}{2}$ state). For the following discussion the simple-minded approximation $\int \sigma dE \sim \Gamma_p\Gamma_\gamma$ is used to compute relative integrated absorption cross sections and Γ_p is taken proportional to the squared coefficient of fractional parentage of the 2h-1p state in terms of $^{14}C+p$ and $^{14}N+p$. This yields 0.004, 1.63, and 0.40 MeV mb for the $T=\frac{3}{2}$ states at 24.3 ($\frac{1}{2}^+$), 24.9 ($\frac{3}{2}^+$), and 25.7 MeV ($\frac{1}{2}^+$) in the $^{14}C+p$ channel, respectively. The capture strength is thus concentrated in one resonance.

It has been suggested that the strong peak at $E_x=20.5$ MeV in the $^{14}C+p$ channel has $T=\frac{3}{2}$ since it appears very weakly in the $^{14}N+p$ channel. This was supported by the calculations of Fraser *et al.*[19] which predict a $J=\frac{3}{2}$ $T=\frac{3}{2}$ state at 21.7 MeV with an integrated absorption cross section of 1.25 MeV mb for the $^{15}N(\gamma,p_0)^{14}C$ reactions. Similarly, Zhusupov and Eramzhian[34] predict such a state at 21.2 MeV with an integrated cross section of 2.6 MeV mb. Both find little $T=\frac{1}{2}$ strength around 20.5 MeV. The present results are different. The nearest $T=\frac{3}{2}$ states at 21.2 and 22.3 MeV have integrated cross sections of 0.0001 and 0.15 MeV mb for the $^{15}N(\gamma,p_0)^{14}C$ reactions. On the other hand, the $T=\frac{1}{2}$ state predicted here at 20.7 MeV ($J=\frac{3}{2}$) has integrated absorption cross sections of 1.7 and 1.0 MeV mb in the $^{14}C+p$ and $^{14}N+p$ channels, respectively (which includes the isospin Clebsch-Gordan factor). It is thus not surprising that the resonance is stronger in $^{14}C+p$ than in $^{14}N+p$, although the data indicate an even bigger ratio. The peak at 19.5 MeV in the $^{14}C+p$ channel has absolutely no counterpart in $^{14}N+p$, and could well have $T=\frac{3}{2}$ character.

Over all, the distribution of collective strength as a whole and of the $T=\frac{1}{2}$ and $\frac{3}{2}$ components in particular, is well explained by the microscopic model. Finally, we emphasize the fact that the strong peak observed in $^{14}C+p$ at 26 MeV is totally absent in $^{14}N+p$. Assuming the $T=\frac{3}{2}$ assignment to be correct, this would indicate a very small degree of isospin mixing at least in this region of the GDR.

C. Region above the GDR

The only feature seen in the excitation function above 27 MeV is a weak but persistent peak at 37 MeV. It is tempting to associate this peak with the $1s_{1/2}$-hole state. This state was not included in the present calculations but is predicted by Fraser *et al.*[19] between 36 and 39 MeV. It carries considerable $E1$ strength but couples only weakly to the $^{14}C+p$ channel. It should be much stronger in the $^{14}N+p$ channel,[19] but lies above the present range of data. This identification is very doubtful, however, since it is known from the results on the (e,ep') reaction[35] and the $(p,2p)$ reaction[36] that the $1s_{1/2}$-hole strength is spread out over about 10 MeV in ^{12}C and ^{16}O.

VI. CONCLUSION

The motivation of this series of papers on $A=17$ and $A=15$ nuclei was to understand the effect which one extra nucleon has on the redistribution of collective electric dipole strengths. The results of I, II, and this paper demonstrate that this is quantitatively understood in the lowest order particle-hole model. The interaction which we have used was tested in both systems on the low-lying $T=\frac{3}{2}$ states (for which center of mass effects do not arise) and found to reproduce the energy spectrum as well as the depleted $E1$ transition strengths. The same interaction also reproduced the $E1$ strength and isospin distribution in the GDR. This is essentially confirmed here in $A=15$ where both the $T=\frac{1}{2}$ and $\frac{3}{2}$ components have been observed. The fact that the isospin splitting is obtained without parameter adjustment in $T_z=\frac{1}{2}$ nuclei differs quantitively from the heavier nuclei such as $A\approx 89$ where the symmetry potential had to be arbitrarily doubled beyond the value obtained directly from effective interaction calculations.[37]

When the microscopic results are translated into an effective symmetry energy[27] $\Delta E=U(T_0+1)/A$ the potential U is found to be much smaller than the 60 MeV established in heavier nuclei, but close to the upper limit established by Leonardi and Lipparini, i.e., $U=28$ MeV in $A=15$ and $A=17$. ^{13}C is another well studied case. From inelastic electron scattering $U=34$ MeV was found and this value is in good agreement with the model calculations.

In summary, it appears that $E1$ excitations and the related isospin splitting are well understood in light nuclei near ^{16}O.

*Work supported in part by the National Science Foundation and U. S. Energy Research and Development Administration.

†Present Address: KVI - Paddepoel, Groningen, The Netherlands.

[1]M. N. Harakeh, P. Paul, and K. A. Snover, Phys. Rev. C 11, 998 (1975).

[2]M. N. Harakeh, P. Paul, and Ph. Gorodetzky, Phys. Rev. C 11, 1008 (1975).

[3]H. M. Kuan, M. Hasinoff, W. J. O'Connell, and S. S. Hanna, Nucl. Phys. A151, 129 (1970).

[4]H. M. Kuan, C. J. Umbarger, and D. G. Shirk, Nucl. Phys. A160, 211 (1971); A196, 634 (1972).

[5]H. R. Weller, R. A. Blue, J. J. Ramirez, and E. M. Bernstein, Nucl. Phys. A207, 177 (1973) and earlier work cited therein.

[6]H. R. Weller, R. A. Blue, J. J. Ramirez, E. M. Bernstein, H. R. Hiddleston, R. M. Prior, S. E. Darden, and M. Divadeenam, Phys. Rev. C 10, 575 (1974).

[7]R. Kosiek, Z. Phys. 179, 544 (1964).

[8]J. D. Garrett, F. Ajzenberg-Selove, and H. G. Bingham, Phys. Rev. C 10, 1730 (1974).

[9]F. C. Young, A. S. Figuera, and C. E. Steerman, Nucl. Phys. A173, 239 (1971).

[10]G. A. Bartholomew, F. Brown, H. E. Gove, A. E. Litherland, and E. B. Paul, Can. J. Phys. 33, 441 (1955).

[11]M. Schaeffer, A. Degrê, S. L. Blatt, and M. Suffert, in *Proceedings of the International Conference on Nuclear Physics, Munich, 1973,* edited by J. De Boer and H. J. Mang (North-Holland, Amsterdam/American Elsevier, New York, 1973); and private communication.

[12]J. J. Murphy, Y. M. Shin, and D. M. Skopik, Bull. Am. Phys. Soc. 20, 628 (1975); Nucl. Phys. A246, 221 (1975).

[13]H. R. Weller, R. A. Blue, J. J. Ramirez, and E. M. Bernstein, Phys. Rev. C 11, 1464 (1975).

[14]A. P. Shukla and G. E Brown, Nucl. Phys. A112, 296 (1968).

[15]A. P. Zuker, B. Buck, and J. B. McGrory, Phys. Rev. Lett. 21, 39 (1968).

[16]S. Lie, T. Engeland, and G. Dahll, Nucl. Phys. A156, 449 (1970).

[17]A. P. Zuker, B. Buck, and J. B. McGrory, BNL Report No. BNL-14085 (unpublished).

[18]M. Soga, Nucl. Phys. 89, 697 (1966).

[19]R. F. Fraser, R. K. Garnsworthy, and B. M. Spicer, Nucl. Phys. A156, 489 (1970).

[20]T. T. S. Kuo (private communication).

[21]S. Cohen and D. Kurath, Nucl. Phys. 73, 1 (1965).

[22]B. Giraud, Nucl. Phys. 71, 373 (1965).

[23]G. W. Phillips, P. Richard, D. O. Elliot, F. F. Hopkins, and A. C. Porter, Phys. Rev. C 5, 297 (1972).

[24]See E. Hayward, Natl. Bur. Stand. Monograph No. 118, 1970 (U. S. Dept. of Commerce).

[25]S. Fallieros and B. Goulard, Nucl. Phys. A147, 593 (1970).

[26]E. Hayward, B. F. Bigson, and J. S. O'Connell, Phys. Rev. C 5, 846 (1972).

[27]R. O. Akŭyz and S. Fallieros, Phys. Rev. Lett. 27, 1016 (1971).

[28]P. Paul, J. F. Amann, and K. A. Snover, Phys. Rev. Lett. 27, 1013 (1971).

[29]R. Leonardi, Phys. Rev. Lett. 28, 836 (1972).

[30]R. Leonardi, and E. Lipparini, Phys. Rev. C 11, 2073 (1975).

[31]J. J. Ramirez, R. A. Blue, and H. R. Weller, Phys. Rev. C 5, 17 (1972).

[32]H. M. Kuan and D. G. Shirk (unpublished).

[33]H. R. Weller, N. R. Roberson, D. Rickel, and D. R. Tilley, Phys. Rev. Lett. 11, 657 (1974).

[34]M. A. Zhusupore and R. A. Eramzhian, as quoted in Ref. 3.

[35]R. E. Wagner (private communication).

[36]U. Wille and R. Lipperheide, Nucl. Phys. A189, 113 (1972).

[37]J. D. Vergados and T. T. S. Kuo, Nucl. Phys. A168, 225 (1971).